v. 1, n. 1, 2024

International Journal of Exact Sciences

EFFECTIVENESS OF THREE FINGERPRINTING TECHNIQUES TO CORRELATE OIL SEEPS: BIOMARKERS, DIAMONDOIDS, AND MULTI-ELEMENTAL ANALYSIS

Elias Kassabji

Bryan Gunawan

Tithi Ghosh

Kyle Wyman Bostick

Jamshid Gharib

HIGHLIGHTS

Comparison between conventional and novel fingerprinting methods.

Evaluation of interference in the results due to recent organic matter content.

Use of multi-element distributions and relative abundances as a correlation tool.

Abstract: Seeped oil-to-source correlation requires sophisticated geochemical fingerprinting techniques and an understanding of their limitations. Through the past several decades, studies have used EOM composition, biomarkers, diamondoids, and multi-elemental analyses to correlate oils in reservoir studies; yet only EOM composition and biomarkers are routinely used to correlate seeped oils. Thus, in the current study, seven seeped oils (Soxhlet-extracted, mainly Type III (terrestrial origin) and Type II/III (mixed) of organic matter in the source rock, API values = 35 - 40°) from a single basin (consisting of five Blocks: A, B, D, E, and F) and EOM from a background sample (from Block C) were analyzed using the aforementioned techniques and data therein was correlated to investigate the utility of these as advanced geochemical seep hunting tools. The extracted oils (from Blocks A, B, D, and E) varied between light condensates and black oils. Variations on the seeped oils may be attributed to oil fractionation, thermal maturation, chemical interactions during the upward migration of hydrocarbons, and / or biodegradation. Biomarkers results confirmed a Tertiary to Late Cretaceous Type III, low hydrogen kerogen source, and Type II/III consisting of high 18a(H)-oleanane (average Ol/H_{30}=0.50), Gammacerane, a high $(C_{29})/(C_{28}+C_{27})$ sterane ratio, and low abundance of C_{30} steranes. Diamondoid analysis complemented these findings by targeting light hydrocarbon compounds, which are biodegraded in areas of passive or microseepage. High adamantane:diamantane ratios were consistently observed across the basin's seeped oil extracts, suggestive of light condensate oil. According to the results, diamondoids are a better indicator of maturity than biomarker parameters, especially for biodegraded hydrocarbons. The study also helped to find relation among elements, which could be of interest in correlating oils from similar/different sources when looking at seeps. Lastly, a logical workflow strategy is provided that can be used to determine which fingerprinting techniques are merited for seeped oil samples.

INTRODUCTION

Historically, hydrocarbon exploration relied on identifying petroleum seeps at the surface, indicating active petroleum systems. Offshore, slicks on the ocean surface and gas bubbles were used for detection. However, geochemical methods have proven more effective over the last century (e.g., Horvitz, 1939; Jones and Drozd, 1983; Brooks and Carey, 1986; Abrams, 2005). Common techniques include solvent extraction, fluorescence, and gas detection in surface sediments. Yet, these methods have limitations, such as interference from recent organic matter, non-fluorescence of small aromatic molecules, and fractionation of gas during sample collection.

To address these limitations, new methods have emerged, including biomarker and diamondoid detection. However, recent organic matter in modern sediments still complicates biomarker analysis. Diamondoids offer valuable insights into source rock and maturity assessment, especially in highly biodegraded and condensate samples. Multi-element analysis, a newer technique, has been used for oil-oil and oil-source rock correlations (e.g., Lewan, 1984; Curiale, 1987; Barwise, 1990). Metals play a crucial role, particularly in biodegraded oil samples

(e.g., Lewan, 1984; Nakada et al., 2010; Zhang et al., 2009). By combining biomarkers, diamondoids, and multi-element analysis, we gain a comprehensive understanding of seeped oil variability.

Our study aims to demonstrate the benefits of integrating these techniques. We evaluate source-to-seep correlations, assess the correlation of oil seepages with severe biodegradation, and explore the applicability of metal data for establishing genetic connections among seeped hydrocarbons. This novel approach leverages trace elements concentrated in nitrogen-, sulfur-, and oxygen-containing components of petroleum, such as metalloporphyrins. As interest grows in the molecular association of metals with heavy and biodegraded oils, these techniques could revolutionize hydrocarbon exploration in the future (Tissot and Welte, 1984; Philp, 1985; Peters et al., 2005; Waples and Machihara, 1991).

GEOLOGICAL BACKGROUND

Samples were collected offshore Malaysia as part of a seep hunting campaign. Figure 1 shows the general location of these samples. In the interest of preserving proprietary information, we have chosen to withhold the exact coordinates that would directly indicate geographic location.

Figure 1 General location map of the study area offshore Malaysia.

The tectonic evolution and formation of the Sabah Basin, offshore Malaysia, have been primarily controlled by fore-arc extension during the Cretaceous to Eocene subduction of the oceanic crust (Tongkul, 1991). The basement of the Sabah Basin comprises a heterogeneous continental terrane with a complex structural origin from a strike-slip and extensional regime, as noted in Tongkul (1991). This Tertiary-fill basin was filled chaotically with bathyal/outer neritic clays and siliceous oozes, neritic sands and carbonates, peaty terrigenous organic matter, and carbonaceous mudstones (Figure 2). The rapid sedimentation was controlled by the steep uplift and subsequent erosion of the associated volcanic arc during the Early to Middle Miocene (Tongkul, 1991).

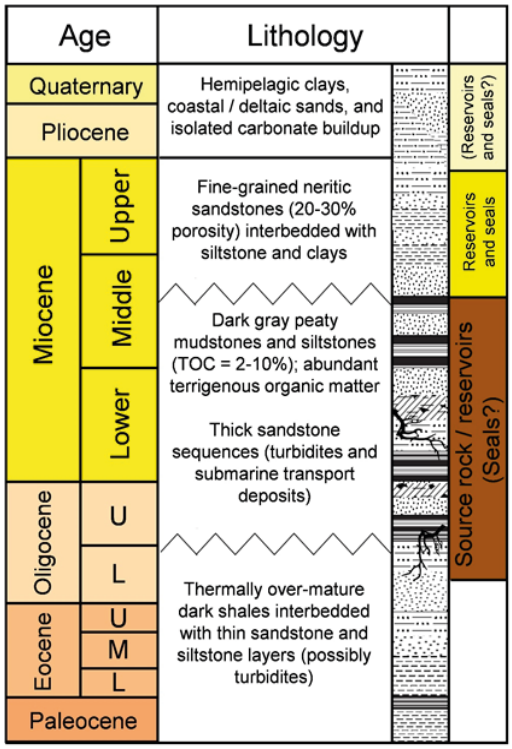

Figure 2 Generalized stratigraphy of the studied basin and potential contributors to petroleum plays. A stylized recreation of published works (e.g., after Tongkul (1991)) is shown instead of the actual basin location for reasons of proprietary confidentiality.

The Sabah Basin has been affected by frequent tectonic uplift and subsidence events (Tongkul, 1991). The deposition of the Miocene mudstones was interrupted by the placement of periodic sandy reservoir-prone facies with high porosity (10-20%) and extensive unconformities due to subaerial exposure (Abdullah et al., 2017). Many of these organic-rich Miocene sediments were thrust downward into the oil and gas window during subsidence events, and fold-thrust dynamics present throughout the Mid-Cenozoic resulted in anticlinal traps and numerous thrust and normal faults, which are considered as potential conduits for petroleum migration and seepage to the seabed (Abdullah et al., 2017).

The primary hydrocarbon source in the Sabah Basin is the Miocene organic-rich sediments, as discussed in Gou (2014). Using coastal outcroppings of these formations, it was found that most of these dark gray siltstone and mudstone source rocks have a vitrinite reflectance of 0.7-1.2%Ro and an average TOC of ~3.5%, but some instances showed TOC values exceeding 10% (Abdullah et al., 2017). The Early Oligocene strata below these sediments were believed to be thermally over-mature, based on heat flow measurements in the region (Abdullah et al., 2017).

The oils produced in the offshore plays of the Sabah Basin are thermally mature (API values=35-40°; CPI (nC_{25} - nC_{31}) =1.0-1.2) and are classified as both non-waxy light and black oils, having n-alkane distributions ranging from C_{11} to C_{34} (max peaks at < nC_{20}), as described in Jamil et al. (1991). The kerogen types of these source rocks have been mainly classified as a mixture of Types II, III, and IV using O- and H-indices, supported by petrographic maceral analysis which showed the source rocks containing abundant fibrous plant fragments, vitrinite, and inertinite (Jamil et al., 1991). The origin of the kerogen was determined to be terrigenous using triterpane and sterane biomarkers in these oils inertinite (Jamil et al., 1991). The high concentrations of 18α(H)-oleanane, a high $(C_{29})/(C_{28}+C_{27})$ sterane ratio, and absence of C_{30} steranes suggest a terrigenous origin (Jamil et al., 1991). Finally, high pristane/phytane ratios (>3.0) and pristane/nC_{17} ratios (>1.0) indicate that the source organic matter was deposited under a sub-oxic environment, such as a peat swamp or coastal wetland (Jamil et al., 1991).

MATERIALS AND METHODS

SURVEYING AND SEEP IDENTIFICATION

A multibeam echosounder technology and subbottom data collection methods was employed. Fugro utilized a Kongsberg EM302 multibeam system for bathymetry, backscatter, and water column data, along with a Kongsberg Subbottom Profiling 300 Echosounder for shallow seismic data.

We focused on features indicative of hydrocarbon seepage, including bathymetric features (mounds, pockmarks, and faults), high-intensity backscatter anomalies, vertical water column anomalies, faulting, and anticlinal structures. Fugro conducted higher-resolution data collection along a 1-km transect at these targets before core collection. To minimize contamination risk, we precisely retrieved piston cores (6 m in length). Significant sediment samples from deeper core sections (4-6 m) were quickly frozen to -80°C upon retrieval.

SEDIMENT EXTRACTION

Thawed frozen samples were air-dried on acid-treated watch glasses. The dried sediment was ground into a fine powder using solvent-washed ceramic mortar and pestles. A Soxhlet apparatus was used with organic solvent (n-Hexane, 95%) and a cellulose thimble filled

International Journal of Exact Sciences ISSN 2966-1153 DOI https://doi.org/10.22533/at.ed.153112401079

with prepared seabed sediment. The samples were extracted for 48 hours (at ~55-60°C) to enhance recoverable extractable organic matter (EOM). Sediment extracts were concentrated using a rotary evaporator and further evaporated in a heating chamber to approximately 1 mL volume, avoiding volatile diamondoid fractionation.

BIOMARKER AND DIAMONDOIDS ANALYSES

Biomarker Analysis:

We analyzed saturated and aromatic hydrocarbons (e.g., phenanthrenes, naphthalenes, and dibenzothiophenes) using a 6890 Agilent GC system with ion mass m/z 191 and m/z 217. The gas chromatograph-mass spectrometer (GC-MS) utilized a 60 m x 250 µm x 0.25 µm capillary dimethylpolysiloxane column. Saturate compounds were analyzed with a temperature program from 145°C to 320°C, while aromatics were analyzed from 70°C to 320°C.

Diamondoids Analysis:

We used an Agilent 7890B/5977 GC-MS system with MassHunter software. An HP1-MS column (60 m, 0.25 mm ID, 250 µm film thickness) was employed. Calibration standards containing n-dodecane-d26 (for adamantanes) and n-hexadecane-d34 (for diamantanes) were added to the extracts. Peak area ratios determined diamondoid concentrations relative to the extract's dry mass and pre-extracted sediment weight. Adamantanes were analyzed at m/z 135, 136, 149, 163, and 177 daltons, while diamantanes were analyzed at m/z 131, 187, 188, 201, and 215 daltons.

MULTI-ELEMENT ANALYSIS

We developed an analytical and calibration methodology using ICP-OES for major, minor, and high-abundance trace elements. The multi-element analysis involved a strong-acid EOM digestion technique using a single reaction chamber microwave to create organic-free, metal-bearing aqueous solutions. A triple-quadrupole ICP-MS determined trace and ultra-trace element concentrations (Casey et al. (2016) and Yang et al. (2017)).

We re-dissolved EOM samples in DCM (Dichloromethane) before transferring them to quartz digestion tubes. The tubes underwent evaporation at 45°C for 3 hours to remove residual DCM. Subsequently, 5 mL of 16N HNO3 was added to each acid digestion tube. The tubes were loaded into the SRC Microwave Digestion System (Model UltraWAVE) for acid digestion. Concentrated nitric acid used for microwave digestion was purified with a PTFE sub-boiling distillation system.

The resulting analytes (digested solution) were evaporated to incipient dryness in clean Teflon vials under a custom-built HEPA-filtered heating chamber for 24-48 hours. After evaporation, the digested samples were re-dissolved with 2% HNO3. Solutions were transferred to pre-weighed Teflon tubes, and their masses were recorded for trace element calculations.

Elemental Analysis:

ICP-OES (Model 725 from Agilent Technologies) analyzed V, Ni, and S.

QQQ-ICP-MS (Model 8800 from Agilent Technologies) analyzed other elements (up to 53).

Trace elements included Al, Mg, Fe, Mn, Ti, Ca, Na, K, and P.

Ultra-trace elements included Li, Be, B, Sc, Ti, V, Cr, Co, Ni, Cu, Zn, Ga, Rb, Sr, Y, Zr, Nb, Cs, Ba, La, Ce, Pr, Nd, Sm, Eu, Tb, Gd, Dy, Ho, Er, Yb, Lu, Hf, Ta, Pb, Th, and U.

Concentrations were calculated based on EOM weight and digested solution weight (dilution ratio), reported as µg g-1 for trace elements and ng g-1 for ultra-trace elements.

RESULTS AND DISCUSSION

We conducted chromatographic analysis on hexane-extracted sediment samples to determine the distribution of C_{15}+ n-alkanes. Visual inspection of chromatograms allowed us to recognize thermogenic hydrocarbons (C_{15}-C_{24}) and recent organic matter (ROM), C_{27}-C_{33} range. Our focus was on extractable organic matter yield (EOM) related to migrated hydrocarbons, with values exceeding 200 µg g-1 dry sediment. Chromatographic data also revealed signs of biodegradation (unresolved complex mixtures, UCM) due to oxidizing near-surface conditions.

Quantification and classification involved determining EOM gravimetrically and calculating UCM using an internal standard (squalane). Samples exhibited varied n-alkane distributions: from background samples with ROM to biodegraded black oil. Most chromatograms displayed patterns related to biodegraded light oil/condensate (Figure 3). All samples had EOM greater than 200 ppm, except for the pilot sample and F-01 (indicating migrated hydrocarbons). A few samples (A-01, B-01, E-01, E-01) had EOM values exceeding 1000 ppm, providing evidence of macro-seepages. UCM values correlated positively with EOM in sediment (Table 1).

Biomarker analysis yielded insights into the origin and maturity of the petroleum system. Specific biomarkers indicated environmental deposition, organic matter type, and probable source rock age. Key parameters are summarized in Table 2.

Additionally, we examined fragmentograms for aromatic compounds and estimated relative amounts. Maturity assessment relied on the MPI calculation proposed by Radke and Welte (1983). Aromatic hydrocarbon levels also served as indicators of seepage.

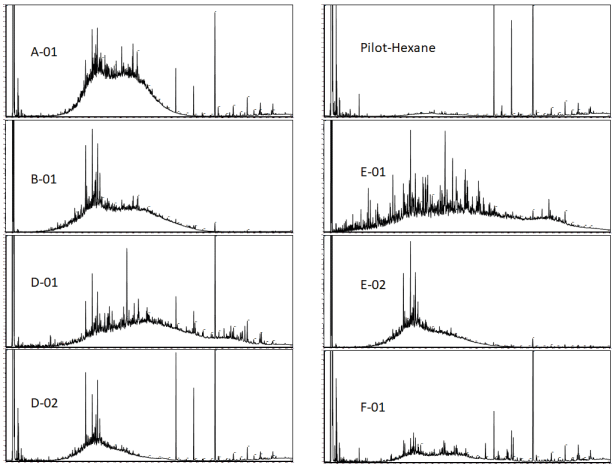

Figure 3 GC-FID traces of total extracts of seabed sediments showing differences in composition. Pilot-hexane exhibits n-alkane distribution dominated by ROM hydrocarbons, (A-01) bimodal UCM-hump, slightly higher in the C_{13}-C_{16} range, (B-01) bimodal UCM-hump, slightly higher in the C_{13}-C_{16} range, (D-01) bimodal UCM-hump, higher in the < C_{23} range, (D-02) unimodal UCM-hump centered in the C_{12}-C_{18} range, (E-01) bimodal UCM-hump, higher in the < C_{23} range, (E-02) unimodal UCM- hump centered in the C_{12}-C_{20} range, and (F-01) Small bimodal UCM-hump in the C_{12}-C_{20} range.

Our analysis reveals varying biomarker distributions in the samples, ranging from ROM-dominated (Pilot-hexane) to black oil and condensate seepage. Specifically, we examined triterpanes and the oleanane index. Triterpanes in m/z 191 exhibit patterns typical of deltaic source rocks, with relative increases in tricyclic terpanes observed in samples with light oil/condensate. The oleanane/C_{30} hopane ratio (oleanane index) indicates higher plant input of Late Cretaceous or younger age (Bagge and Keeley , 1994; Riva et al., 1988). Notably, blocks D and E show a higher oleanane index, corresponding to a bimodal hump of UCM with varying molecular

International Journal of Exact Sciences ISSN 2966-1153 DOI https://doi.org/10.22533/at.ed.153112401079

Sample	Block	Sample Description	EOM (mg g^{-1} dry sediment)	UCM (mg g^{-1} dry sediment)	Classification
Pilot-Hexane	C	Greenish gray soft clay	94.51	86.85	Background
A-01	A	Greenish gray firm clay w/ carbonate ooze and abundant gas hydrate	1029.90	1008.42	Biodegraded light oil/ condensate
B-01	B	Dark greenish-gray soft clay	2928.12	2898.72	Biodegraded light oil/ condensate
D-01	D	Greenish gray soft clay	246.88	236.31	Biodegraded black oil
D-02	D	Greenish gray soft clay	308.42	292.32	Biodegraded light oil/ condensate
E-01	E	Greenish gray soft clay	6165.49	6103.35	Biodegraded black oil
E-02	E	Greenish gray soft clay	820.99	804.57	Biodegraded light oil/ condensate
F-01	F	Greenish gray soft clay	117.67	106.10	Relic biodegraded light oil/condensate

Table 1 Gas chromatography properties of the marine sediments.

Parameters	Pilot-Hex.	A-01	B-01	D-01	D-02	E-01	E-02	F-01
TTC_{22}/C_{21}	0.63	0.52	1.02	1.09	0.56	0.74	0.65	0.73
Ts/(Ts+Tm) (%)	76.38	51.30	44.49	47.22	56.10	52.08	53.19	40.57
H_{29}/H_{30}	0.09	0.31	0.17	0.48	0.59	0.39	0.65	0.37
Ol/H_{30}	0.11	0.34	bdl	1.14	0.10	1.59	0.23	0.30
Ster/Hop	0.14	0.07	0.24	0.28	0.19	0.20	0.21	0.37
$SterC_{27}/C_{29}$	1.33	bdl	1.16	0.71	0.61	0.70	0.61	1.34
$\%C_{27}$	42.44	82.63	44.69	30.96	30.19	24.83	25.10	45.60
$\%C_{28}$	25.61	17.37	16.70	25.65	20.67	39.71	33.96	20.35
$\%C_{29}$	31.95	bdl	38.61	43.39	49.14	35.45	40.94	34.05
MPI	0.84	bdl	bdl	1.03	0.52	1.08	0.47	0.99
%Ro_equiv.	0.90	0.40	bdl	1.02	0.71	1.05	0.68	1.00

Table 2 Biomarker key parameters for saturates and aromatic hydrocarbons.

TTC_{22}/C_{21} : Tricyclic terpane C_{22}/C_{21}

Ts/(Ts+Tm): 18α-22, 29, 30-trisnorneohopane (Ts) and 17α-22, 29, 30-trisnorhopane (Tm) ratio

H_{29}/H_{30} : Hopane C_{29} versus Hopane C_{30}

Ol/H_{30} : 18a(H) Oleanane (Ol) versus Hopane C_{30}

Ster/Hop: Steranes versus hopanes

$SterC_{27}/C_{29}$: Steranes C_{27} versus Steranes C_{29}

$\%C_{27}$, $\%C_{28}$, $\%C_{29}$: Relative abundance of regular steranes

MPI: Methylphenanthrene index

%Ro_equiv.: Equivalent reflectance vitrinite based on MPI.

Bdl: below the detection limit

weight. Moreover, gammacerane, present in low concentrations, suggests a low salinity depositional environment (Peter et al., 2005).

Sterane analysis reveals a predominance of terrigenous C_{29} to C_{27} regular steranes. Blocks A, B, C (Pilot-Hexane), and F exhibit lower concentrations of thermogenic biomarkers, complicated by ROM interference (Dembicki, 2010). Immature compounds are noticeable in m/z 191 and 217, influenced by ROM and contributing to the low maturity of the least biodegraded samples.

Additionally, a typical ternary plot for regular steranes (Figure 4) sheds light on likely source types. Blocks D and E share organic matter types associated with a terrestrial source (Shanmugam, 1985), similar to known source rock extracts. In contrast, blocks A, B, C (Pilot-Hexane), and F exhibit a more transitional organic matter type, possibly influenced by ROM and low thermogenic biomarker concentrations.

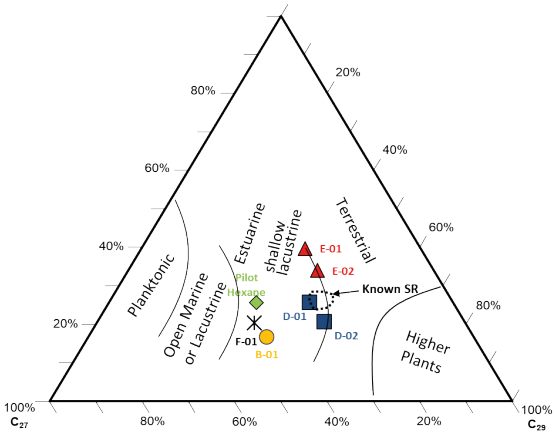

Figure 4 Ternary plot for interpretation of regular steranes distributions regarding organic matter source. Interpretation template modified from Shanmugam, 1985. Samples are plotted together with the source rock extract result (SR-extract, black dot) to show the seeped hydrocarbons' potential correlation.

Aromatic compounds, including naphthalenes, phenanthrenes, and dibenzothiophenes, play a crucial role in identifying the origin of hydrocarbons. Their presence in rock or oil samples (ROM) indicates that the hydrocarbons likely come from reworked materials. However, there are challenges. Naphthalenes have a low boiling point, which can lead to their loss during sample preparation. Additionally, aromatic compounds are more soluble in water than saturated components, making them susceptible to removal during migration.

The abundance of phenanthrene in samples suggests moderately mature hydrocarbons. The methyl phenanthrene index (MPI) is particularly useful for oils originating from terrestrial kerogen sources. The maturity level of the samples based on MPI ranges between 0.7 and 1.0%Ro, including those classified as having condensate-like hydrocarbons. However, limitations exist. Aromatics may be lost during extraction and evaporation, affecting the ratios used for maturity assessment. As a result, the maturity assessment based solely on MPI is inconclusive. To better understand the thermal maturity of these seeped hydrocarbons, additional parameters such as diamondoid must be considered.

The diamondoid analysis, conducted using the same extracts as the biomarker analysis, provides valuable insights that complement our understanding of sourcing and maturity. Key diamondoid parameters are summarized in Table 3.

Firstly, the concentration of diamondoid compounds exhibits significant variation across all samples. This concentration closely correlates with the extractable organic matter (EOM) content and, consequently, the volume of seeped hydrocarbons. The pilot sample serves as a baseline, establishing the background level of diamondoids in the study area. This background level likely

results from reworked material (Piggott and Abrams, 1996) and contains approximately 12.5 ppm of total diamondoids—a value similar to marine background levels reported by Dahl et al. (1999). Notably, sample F-01, located farther east in the study area, shows comparable diamondoid concentrations (13.0 ppm), serving as an example of reworked or low-thermogenic materials. Other samples exhibit higher total diamondoid amounts (>25 ppm), consistent with larger EOM and oil-like signatures.

Secondly, the distribution of adamantanes relative to diamantanes is a notable feature. All samples except for A-01-2 have a high proportion of adamantanes. Localized evaporation likely enriches the upper section (A-01-1) in adamantanes, while the lower section (A-01-2) lacks them.

Lastly, the relatively higher adamantane-to-diamantane ratio may be linked to the predominant light oil/condensate seepage type in the area. Interestingly, sediment samples B-01 (light oil) and E-01 (black oil) did not yield measurable diamantanes. The fragmentograms for diamantanes were broad and diffused, likely due to sample characteristics. Notably, B-01 and E-01 had significantly greater recovered EOM quantities (223.4 mg and 334.3 mg, respectively) compared to other sediment samples (ranging from 9.1 to 78.5 mg). The exact reason for this difference remains unclear.

Diamondoids play a crucial role in understanding organic facies and source rock types. By analyzing diamondoid distributions in solvent extracts from marine siliciclastic shales, marine carbonates, and coals, researchers can gain insights into the hydrocarbon source. For instance, the formation of specific diamondoids—such as 3,4-dimethyldiamantane (DMD), 4,8-DMD, and 4,9-DMD—has been linked to specific sources (as demonstrated by Schulz et al., 2001, and Wei et al., 2006). These compounds allow us to distinguish between terrigenous, marine carbonate, and marine siliciclastic facies.

In Figure 5, we present a ternary plot showing the relative abundances of 3,4-DMD, 4,8-DMD, and 4,9-DMD for all samples. Notably, there is a cluster of samples corresponding to Kerogen Type II/III. This cluster represents a mixture of marine and terrigenous organic matter, as described by Schulz et al. (2001). Regardless of the oil type, the relative amounts of DMDs suggest a consistent source for the seeped hydrocarbons in the area.

We can also evaluate oils composed of mixtures of high and low maturity components. Dahl et al. (1999) demonstrated that the decrease in stigmastanes (a type of biomarker) correlates with the increase in 3- and 4-methyldiamantanes due to maturity increase or thermal cracking. Interestingly, the stigmastanes concentration in most samples is low, except for samples D-01 and E-01 (black oils). In these cases, the low stigmastanes concentration may result from higher maturity in the condensate-like samples, as depicted in Figure 6. Notably, sample A-01-1 appears to be intensely cracked compared to the other samples, suggesting potential secondary cracking occurring in a deep-seated reservoir.

	Samples								
Parameters	**Pilot-Hexane**	**A-01-1**	**A-01-2**	**B-01**	**D-01**	**D-02**	**E-01**	**E-02**	**F-01**
Total Adamantanes mg g^{-1}	9.25	932.05	4.36	132.85	55.00	31.99	620.29	372.56	10.26
Total Diamantanes mg g^{-1}	3.31	302.16	21.58	bdl	52.32	12.30	bdl	157.37	2.75
MAI (%)	37.73	36.41	44.75	50.74	45.89	54.37	36.84	57.10	59.24
EAI-1	0.30	0.33	0.36	0.29	0.27	0.30	0.35	0.36	0.39
TMAI-1	0.14	0.21	0.21	0.36	0.33	0.41	0.28	0.46	0.62
MA/A	5.83	12.25	7.72	5.89	4.69	5.45	9.69	10.41	6.98
A/D	0.12	0.11	0.02	bdl	0.42	0.62	bdl	0.55	1.57
MD/D	3.69	4.34	7.46	bdl	5.35	5.09	bdl	7.73	20.06
MDI (%)	45.75	45.22	34.31	bdl	31.40	47.18	bdl	39.81	17.01
DMA/MD	0.19	0.79	0.04	bdl	0.48	1.29	bdl	1.64	1.31

Table 3 Diamondoid key parameters for adamantanes and diamantanes.

MAI (%): Methyladamantane index

EAI-1: Methyldiamantane index

TMAI-1: Trimethyladamantane Index

MA/A: Methyladamantane/adamantane

A/D: Adamantane/diamantane

MD/D: Methyldiamantane/diamantane

MDI (%): Methyldiamantane index

DMA/MD: Dimethyladamantane/methyldiamantane

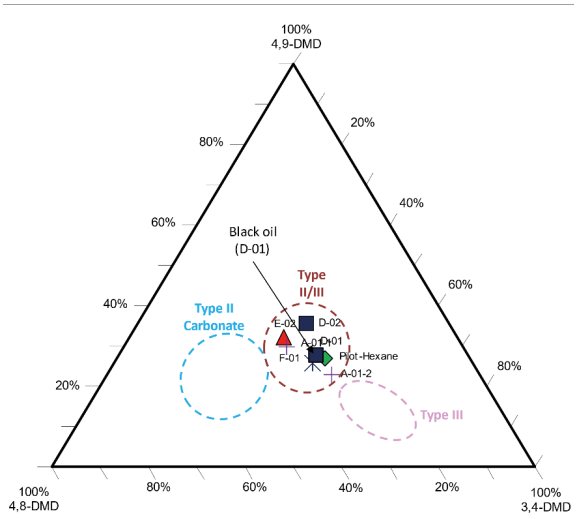

Figure 5 Ternary plot of the relative abundance of 3,4-DMD, 4,8-DMD, and 4,9-DMD illustrating the different organic facies (interpretation after Schulz et al., 2001).

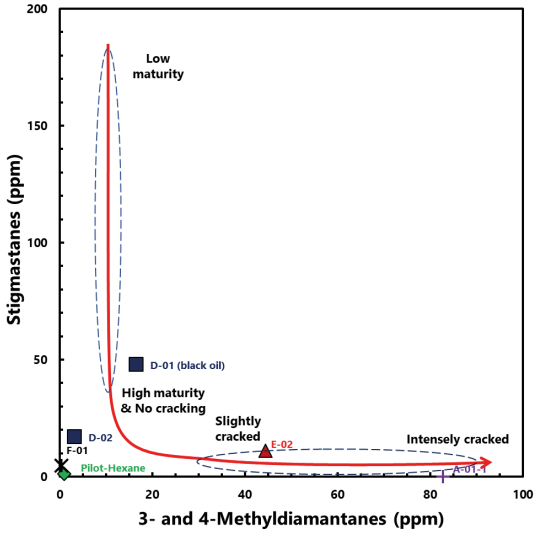

Figure 6 Cracking and mixed oil characteristics utilizing the concentration of stigmastanes (Biomarker) and methyldiamantanes (Diamondoid). Interpretation template after Dahl et al. (1999).

The resistance of diamondoids to both thermal and biological alteration makes them valuable indicators. Specifically, the concentration of ethyl adamantanes undergoes changes in the late gas window maturity range (as observed by Schulz et al., 2001). In contrast, compounds like dimethyl diamantane remain largely unaffected by maturity. Evaluating maturity beyond the oil window stage can be challenging using biomarker parameters alone. Once they reach equilibrium values within the oil window equivalent range, these parameters become insensitive to further thermal maturation, even for various isomerization ratios of molecular biomarkers.

Two commonly used diamondoid hydrocarbon ratios help assess maturity in oil and source rock samples:

1. Methyl Adamantane Index (MAI):
Calculated as

1-MA/(1-MA+2-MA)

2. Methyl Diamantane Index (MDI):
Calculated as

4-MD/(1-MD+3-MD+4-MD)

(%) MAI and (%) MDI increase with increasing maturity (Chen, et al., 1996). Using MAI and MDI we note that for black oil (D-01), the indices indicate peak oil with a maturity equivalent of 1.1% Ro, whereas for condensate (D-02), the ratio suggests gas condensate with a maturity equivalent of 1.6% Ro (Figure 7). Diamondoids, being more sensitive to maturity, provide better insights into the maturity level of seeped hydrocarbons compared to biomarker parameters—especially in cases of severe biodegradation.

In summary, diamondoids offer a valuable alternative for assessing maturity beyond the oil window, enhancing our understanding of hydrocarbon sources and their thermal evolution.

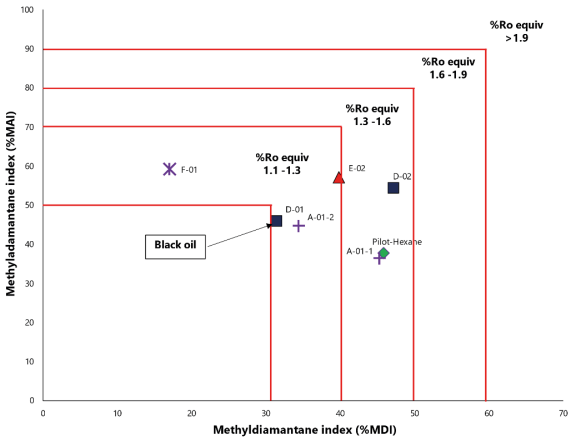

Figure 7 Maturation assessment based on methyladamantane index (%MAI) and methyldiamantane index (%MDI). Interpretation template after Chen et al. (1996)

The multi-element analysis performed on the extracts reveals the composition of 53 elements, including 22 trace elements (with concentrations between 1 and 1000 ppm) and 31 ultra-trace elements (with concentrations below 1 ppm). Abundances of recovered extractable organic matter (EOM) and elemental ratios are summarized in Table 4. Spider diagrams in Figure 8 illustrate the normalized concentration of ultra-trace elements, allowing to fingerprint each seeped hydrocarbon for geographic distribution.

The elements measured in our study fall into two groups: trace elements and ultra-trace elements. The trace elements include Li, B, Na, Mg, Al, P, K, Ca, Ti, V, Cr, Mn, Fe, Co, Ni, Cu, Zn, Se, Rb, Sr, Sn, and Ba. Meanwhile, the ultra-trace elements consist of Be, Sc, Ga, Ge, As, Nb, Cd, Sb, Cs, La, Ce, Pr, Nd, Sm, Eu, Gd, Tb, Dy, Ho, Er, Tm, Yb, Lu, Hf, W, Pb, Th, Y, Zr, Mo, and U.

Surprisingly, sample F-01 exhibits the highest abundance of trace and ultra-trace elements despite having the lowest EOM amount (117 ppm). This discrepancy may result from low EOM concentration and potential errors in the dilution factor. Therefore, caution is advised when

Parameters	A-01-1	A-01-2	B-01	D-01	D-02	E-01	E-02	F-01
Total trace elements μg g^{-1} EOM	113	531	654	4857	859	260	184	4431
Total ultra-trace elements ng g^{-1} EOM	80	613	262	2079	406	149	335	9208
V/Ni	0.01	0.07	0.10	1.05	0.48	0.11	0.40	0.82
V/(V+Ni)	0.01	0.06	0.09	0.51	0.32	0.10	0.28	0.45
Co/Ni	0.01	0.02	0.13	0.07	0.15	0.15	0.21	0.06
Ni/V	102.74	14.89	10.19	0.96	2.1	9.45	2.51	1.22
Mn/Al	0.03	0.02	0.01	0.01	0.01	0.01	0.01	0.01

Table 4 Ratio of selected trace and ultra-trace elements for each sample. For ultra-trace elements, normalized values were used.

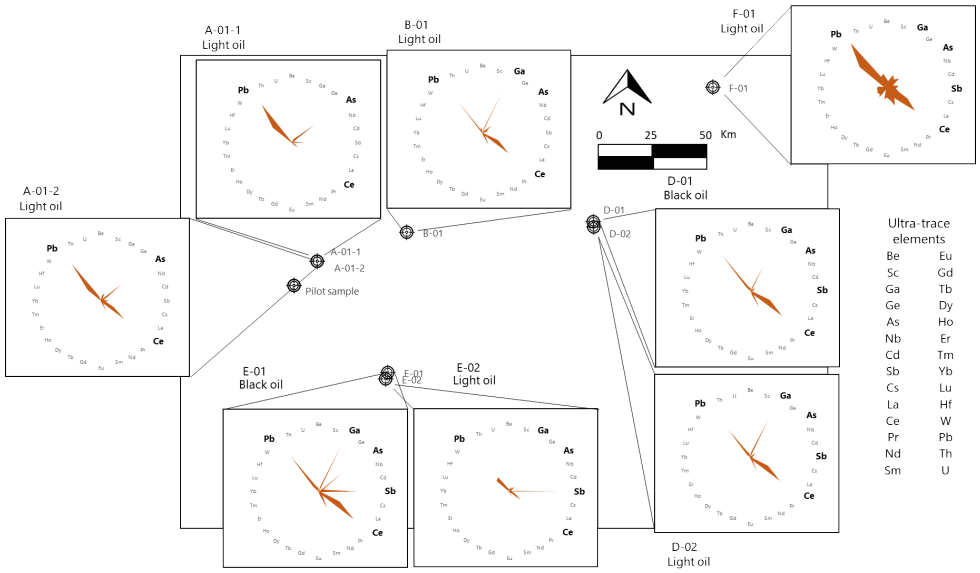

Figure 8 Relative geographical distribution of 28 ultra-trace elements normalized to a 100% total represented in radar diagrams for each sampling site.

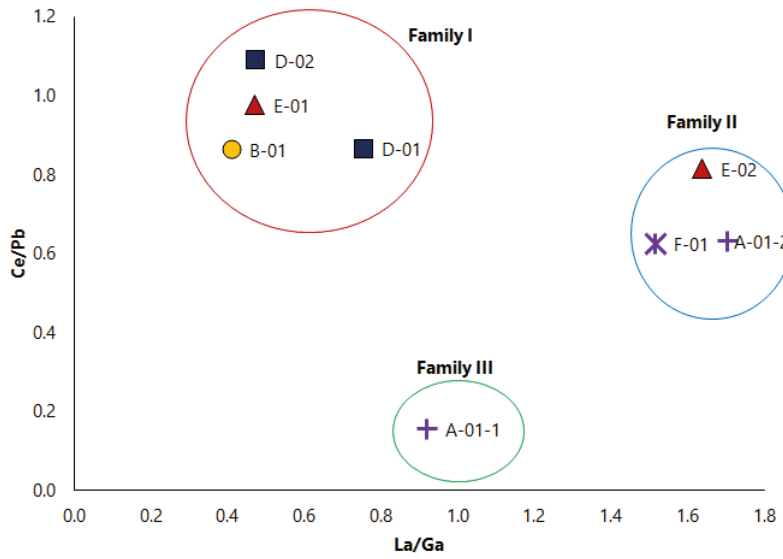

Figure 9 Relationship between Ce/Pb and La/Ga ratios to identify seeped oil families.

interpreting the absolute abundance results from F-01. Samples with very low EOM (<200 ppm), such as the pilot-hexane samples, were excluded due to unreliable data caused by high background-to-signal ratios.

The analysis of the sediment samples revealed that the EOM was enriched in certain trace elements, including Na, Mg, Al, Ca, Cr, Fe, and Se, compared to other elements. Specifically, samples from blocks A, F, and E-02 showed higher concentrations of Fe and Se, with variations in B, Na, Mg, Al, P, K, and Ca. In contrast, samples from blocks B, D-01, and E exhibited a prevalence of Ca as the predominant element, along with lower concentrations of transition metals (Al and Mg). The differential distribution of these elements may be attributed to processes such as adsorption from pore water, seawater, sedimentary layers, and preferential leaching of marine sediments. Additionally, oils with higher terrigenous input tend to have lower metal abundances (Barwise, 1990). Consequently, samples from blocks B, D-01, and E likely have a higher proportion of terrigenous input in their EOM. The trace elements abundance in the extracts appears to be driven by the sediment matrix, therefore the interpretation will be focus on the ultra-trace elements as shown in Figure 8.

In Figure 8, samples B-01, D-01, D-02, and E-01 exhibit a similar distribution of ultra-trace elements. The relative concentration of Pb, Ga, As, and Ce are similar which suggests a common thermogenic hydrocarbon source for these four samples. Other samples show variations from the original fingerprint, likely due to secondary alterations during migration.

Figure 9 shows the relationship between the ratios Ce/Pb and La/Ga which showed significant variation among the samples. The relationship of these ratios confirms the similar ultra-trace distribution of few samples and allowed the identification of three families; Family I represented by samples B-01, D-01, D02, and E-01, Family II comprised by E-02, A-01-2, and F-01, and Family III with only sample A-01-1.

Interestingly, samples A-01-1 and A-01-2, which originate from the same location but at different depths have slight differences in the relative content of Ce which may be attributed to the migration process rather than differences in the source.

We also explored the use of vanadium (V) and nickel (Ni) for crude oil classification and correlation. These elements form metallo-organic bonds in oil, particularly in the higher molecular weight fraction (e.g., porphyrins) (Filby, 1975). The V/Ni ratios remain relatively stable during temperature changes within the oil window or near-surface biodegradation. However, at higher maturities (e.g., condensate range), de-metallization significantly affects these ratios, lowering them (Gao et al., 2017). Figure 10 illustrates the V/Ni vs. V/(V+Ni) diagram, where natural crude oils fall along a forced correlation line. Our samples exhibit a wide range of ratios, with D-01 (black oil) being the least mature hydrocarbon compared to the others. The V/Ni ratio varies significantly across the samples, ranging from 0.01 to 1.05.

Sample E-01, classified as black oil, surprisingly aligns with light oil/condensate samples. This unexpected similarity could be attributed to hydrocarbon migration. During migration, vanadium (V) within asphaltene may adsorb back into the rock, leading to a decrease in the V/Ni ratio over time (Zhou, 1983). Consequently, sample E-01 likely represents a migrated hydrocarbon. The varying V/Ni ratios in other samples may also result from natural oil fractionation during migration.

The Ni/V ratio is also useful for understanding the depositional environment. A value greater than 2 suggests a lacustrine

International Journal of Exact Sciences ISSN 2966-1153 DOI https://doi.org/10.22533/at.ed.153112401079

environment (Lewan, 1984). Based on the Ni/V ratios in Table 4, most samples indicate a lacustrine environment, except for D-01, which hints at a more open marine setting. Moreover, a Co/Ni ratio ≤ 0.1 signifies a terrigenous source rock (Udo et al., 1992). In our samples, except for E-02 and E-01, the rest exhibit terrigenous characteristics. Mn/Al ratio around 0.01 indicates a suboxic condition (Borowski et al., 1999). Most samples align with suboxic conditions, except A-01-1 and A-01-2, which suggest an oxic depositional environment.

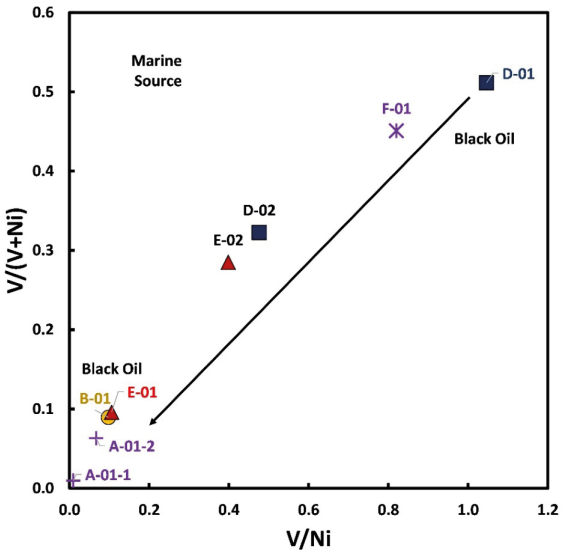

Figure 10 V/Ni vs. V/(V+Ni) plot for all samples. D-01 and E-01 are black oils, whereas the rest of the samples are light oil/condensate. Usually, low ratios values may represent increasing thermal maturity, as shown. Variation of this trend may be ascribed to different hydrocarbon maturity or source rock characteristics.

In summary the use of trace metal, particularly ultra-trace metal aid to complement the source and maturity assessment provided by traditional analytical techniques such as biomarker and diamondoids, especially when addressing highly biodegraded seeped oil.

PROPOSAL FOR AN ENHANCED ANALYTICAL WORKFLOW FOR OIL SEEP SAMPLES

Current fingerprinting strategies often overlook technique limitations. To address this, we propose a logical approach that compares three key analyses (Figure 11): biomarkers, diamondoids, and multi-element distribution. By doing so, we can determine which fingerprints are most valuable for seeped oil samples. Additionally, advanced fingerprinting techniques can help fill gaps in our understanding of composition, source, history, and correlation of seeped oils.

ANALYTICAL WORKFLOW:

Sample Preparation:

- Dry the sediment sample in a clean oven at 40°C for 24 hours.
- Perform solvent extraction using hexane as the organic solvent.

Gas Chromatography (GC) Analysis:

- Determine the distribution of n-alkanes and the amount of extractable organic matter (EOM).
- A chromatogram showing natural n-alkanes without unresolved complex mixture (UCM) development and low EOM content (<200 ppm) is considered a background sample. No further advanced analysis is necessary for such samples.
- For samples containing higher EOM amounts (>200 ppm) but lacking a thermogenic signature on the chromatogram, the same recommendation applies.

Integrated Approach:

- Combine biomarker, diamondoid, and multi-element analyses to identify the possible source of biodegraded oil samples.
- Samples with a thermogenic signature and EOM value exceeding 200 ppm warrant advanced analysis.
- Fresh or unaltered mid to heavy hydrocarbons benefit from biomarker analysis, as it reveals crucial oil source information.
- Incorporate diamondoid analysis to address sourcing and maturity, especially for light hydrocarbons.

This refined workflow ensures a comprehensive assessment of oil seep samples, enhancing the understanding of their composition and origin.

CONCLUSIONS

Surface sediment samples present challenges in analyzing seeped hydrocarbons. While biomarker analysis provides initial insights, it falls short for lighter hydrocarbon compounds. To address this, we propose integrating complementary techniques such as diamondoids and multi-elemental analysis. These approaches enhance correlation and offer new insights into sourcing and maturity. Future studies should explore consistent ratios as proxies for these parameters.

ACKNOWLEDGEMENTS

The authors express their gratitude to FUGRO for the financial support and sample provision, and to the University of Houston for their assistance with the analyses.

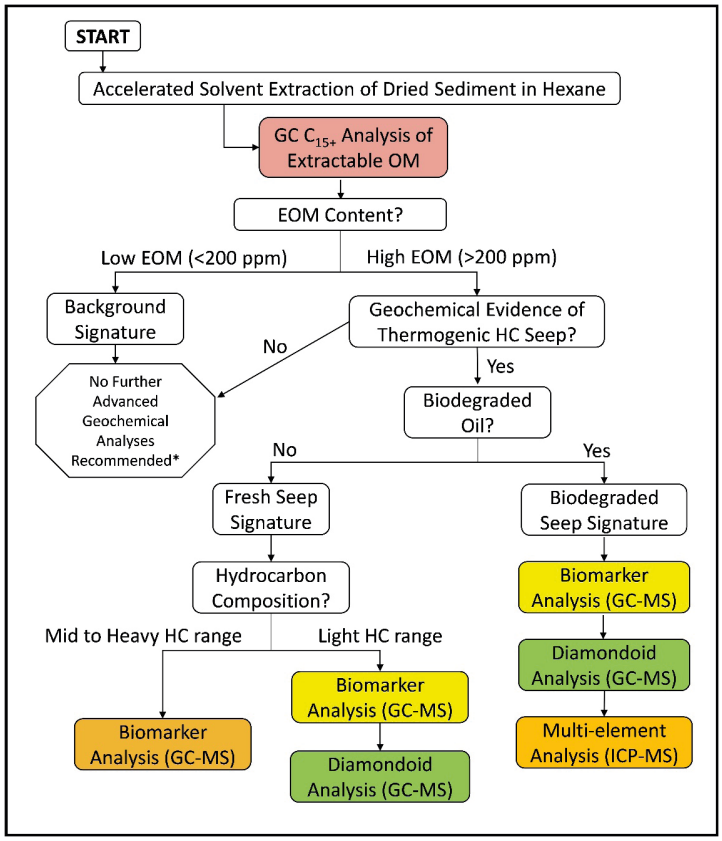

Figure 11 Analytical workflow methodology proposed for analyzing oil seep samples. *While advanced analyses may be unnecessary for samples with either low EOM or no evidence of seepage, these samples could be used as environmental background samples.

REFERENCES

Abdullah, W. H., Togunwa, O. S., Makeen, Y. M., Hakimi, M. H., Mustapha, K. A., Baharuddin, M. H., ... & Tongkul, F. 2017. Hydrocarbon source potential of Eocene-Miocene sequence of western Sabah, Malaysia. Marine and Petroleum Geology, 83, 345-361.

Abrams, M. A. 2005. "Significance of hydrocarbon seepage relative to sub-surface petroleum generation and entrapment." Marine and Petroleum Geology Bulletin, 22-4, 457-478.

Bagge, M.A. and Keeley, M.L., 1994. The oil potential of Mid-Jurassic coals in northern Egypt. Geological Society, London, Special Publications, 77(1), pp.183-200.

Barwise, A. J. G. 1990. "Role of nickel and vanadium in petroleum classification." Energy Fuels 4, 647–652.

Borowski, W. S., Paull, C. K. & Ussler, W. III 1999. "Global and local variations of interstitial sulfate gradients in deep-water, continental margin sediments: Sensitivity to underlying methane and gas hydrates." Mar. Geo. 159, 131–154.

Brooks, J.M. & B. D. Carey. 1986. "Offshore surface geochemical exploration." Oil and Gas Journal, 84, 66-72.

Casey J.F., Gao Y., Yang W. & Thomas R. 2016. "New approaches in sample preparation and precise multi-elementanalysis of crude oils and refined petroleum products using single-reaction-chamber microwave digestion and Triple-Quadrupole ICP-MS." Spectroscopy 31(10), 11-22.

Chen, Junhong, Jiamo Fu, Guoying Sheng, Dehan Liu, and Jianjun Zhang. 1996. "Diamondoid Hydrocarbon Ratios : Novel Maturity Indices for Highly Mature Crude Oils." Organic Geochemistry 25: 179–90.

Curiale, J. A. 1987. "Distribution and Occurrence of Metals in Heavy Crude Oils and Solid Bitumens-Implications for Petroleum Exploration": Section II. Characterization, Maturation, and Degradation. In: R.F. Meyer (Editor), Exploration of Heavy Crude Oil and Natural Bitumen. Am. Assoc. Pet. Geol., Stud. Geol., 25: 207-219.

Dahl, J.E., Moldowan, J.M., Peters, K.E., Claypool, G.E., Rooney, M.A., Michael, G.E., Mello, M.R. and Kohnen, M.L., 1999. Diamondoid hydrocarbons as indicators of natural oil cracking. Nature, 399(6731), pp.54-57.

Dembicki Jr, H., 2010. Recognizing and compensating for interference from the sediment's background organic matter and biodegradation during interpretation of biomarker data from seafloor hydrocarbon seeps: An example from the Marco Polo area seeps, Gulf of Mexico, USA. Marine and petroleum geology, 27(9), pp.1936-1951.

Filby R. H. 1975. "The nature of metals in petroleum." In the Role of Trace Elements in Petroleum (ad. T. F. YEN), pp. 31-58. Ann Arbor Science Publishers Inc., Ann Arbor.

Gao Y., Casey J. F., Bernardo l. M., Yang W. and Bissada K. K. 2017. "Vanadium isotope composition of crude oil: effects of source, maturation, and biodegradation." Geological Society, London, Special Publications, 468, 83-103.

Gou, P. 2014. "Organic petrographic characteristics of the Crocker Formation, NW Sabah, Malaysia." Bulletin of the Geological Society of Malaysia, v. 60, pp. 65-75

Horvitz, L. 1939. "On geochemical prospecting, Geophysics" 4, 210-228.

Jamil, A. S. A.; Anwar, M. L.; Kiang, E. S. P. 1991. "Geochemistry of selected crude oils from Sabah and Sarawak." Geological Society of Malaysia, Bulletin 28, pp. 123-149

Jones, V. T. and R. J. Drozd. 1983. "Predictions of oil and gas potential by near surface geochemistry." American Association Petroleum Geology Bulletin, 67, 932-952.

Lewan, M. D. 1984. "Factors controlling the proportionality of vanadium to nickel in crude oils." Geochimica et Cosmochimica Acta 48, 2231–2238.

Nakada, R., Takahashi, Y., Zheng, G., Yamamoto, Y. & Shimizu, H. 2010. "Abundances of rare earth elements in crude oils and their partitions in water." Geochem. J. 44, 411–418.

Peters, K.E., Walters, C.C., Moldowan, J.M. 2005. "The Biomarker Guide, second ed. Biomarkers and Isotopes in Petroleum Exploration and Earth History." vol. 2. Cambridge University Press, Cambridge. 683 p.

Philp, R P. 1985. "Fossil fuel biomarkers." Elsevier, New York-United States.

Piggott, N., & Abrams, M.A. 1996. Near surface coring in the Beaufort and Chukchi Seas, Alaska. In: American Association Petroleum Geology Memoir No. 66; Schumacher, D., Abrams, M.A., Eds.; American Association of Petroleum Geologists: Tulsa, OK, USA, pp. 385–400.

Radke, M. and Welte, D. H. 1983. "The Methylphenanthrene Index (MPI): a maturity parameter based on aromatic hydrocarbons." In: Bjorøy, M. et al. (eds.), Advances in organic geochemistry 1981. Wiley. Chichester.

Riva, A., Caccialanza, P. G., & Quagliaroli, F. 1988. "Recognition of 18β (H) oleanane in several crudes and Tertiary-Upper Cretaceous sediments. Definition of a new maturity parameter." Organic Geochemistry, 13(4-6), 671-675.

Schulz, Linda K, Arnd Wilhelms, Elin Rein, and Arne S Steen. 2001. "Application of Diamondoids to Distinguish Source Rock Facies." Organic Geochemistry 32 (3): 365–75.

Shanmugam, G. 1985. "Significance of coniferous rain forest and related organic matter in generating commercial quantities of oil, Gippsland Basin, Australia." AAPG Bull., V. 69, No. 8, p. 1241-1254.

Tissot, B. P., & Welte, D. H. 1984. "Geochemical fossils and their significance in petroleum formation. In Petroleum formation and occurrence". (pp. 93-130). Springer, Berlin, Heidelberg.

Tongkul, F. 1991. Tectonic evolution of Sabah, Malaysia. Journal of Southeast Asian Earth Sciences, 6(3-4), 395-405.

Udo, O.T., Ekwere, S., and Abrakasa, S. 1992. "Some trace metal in selected Niger Delta crude oils: application in oil–oil correlation studies." Journal of Mining and Geology 28, 289–291.

Waples, D. W., & Machihara, T. 1991. "Biomarkers for geologist." vol 9. AAPG methods in exploration series. American Association of Petroleum Geologists, Tulsa, 91-99.

Wei, Zhibin, J. Michael Moldowan, Daniel M. Jarvie, and Ronald Hill. 2006. "The Fate of Diamondoids in Coals and Sedimentary Rocks." Geology 34 (12): 1013–16.

Yang, W., Casey, J.F. and Gao, Y., 2017. "A new sample preparation method for crude or fuel oils by mineralization utilizing single reaction chamber microwave for broader multi-elementanalysis by ICP techniques." Fuel 206: 64-79. https://doi.org/10.1016/j.fuel.2017.05.084

Zhang, L., Zhao, Y., Jin, Z., Bai, G., and Yang, L. 2009. "Geochemical characteristics of rare earth elements in petroleum and their responses to mantle-derived fluid: an example from the Dongying Depression, East China." Energy Explor. Exploit. 27, 47–68.

Zhou J.T. 1983. "Distribution feature of trace elements in crude oil from the southern of Songliao basin and the identification of hydrocarbon migration." Journal of Daqing Petroleum Institute 2(18), 44-53 (in Chinese with English abstract).